An analytically solvable model of the effect of magnetic breakdown on angle-dependent magnetoresistance in a quasi-two-dimensional metal

Andrzej Nowojewski,* Paul A. Goddard, and Stephen J. Blundell†
Clarendon Laboratory, University of Oxford, Parks Road, Oxford OX1 3PU, United Kingdom
(Dated: February 3, 2008)

We have developed an analytical model of angle-dependent magnetoresistance oscillations (AMROs) in a quasi-two-dimensional metal in which magnetic breakdown occurs. The model takes account of all the contributions from quasiparticles undergoing both magnetic breakdown and Bragg reflection at each junction and allows extremely efficient simulation of data which can be compared with recent experimental results on the organic metal κ-(BEDT-TTF)$_2$Cu(NCS)$_2$. AMROs resulting from both closed and open orbits emerge naturally at low field, and the model enables the transition to breakdown-AMROs with increasing field to be described in detail.

The measurement of angle-dependent magnetoresistance oscillations (AMROs) is a powerful technique in the determination of details of the Fermi surfaces (FSs) in various reduced-dimensionality metals [1, 2, 3, 4]. In many cases the angle-dependence originates in correlations in the time-dependent interplanar velocity of quasiparticles which traverse the FS under the influence of the magnetic field B and hence can be efficiently simulated by integrating up such correlations for all quasiparticle trajectories [5, 6, 7, 8, 9, 10, 11]. In high B, the additional effect of magnetic breakdown (MB) can *substantially* complicate this picture. This effect occurs in the FSs of quasi-two-dimensional metals such as that illustrated in Fig. 1(a) which is described by the dispersion $E(k) = \hbar^2(k_x^2 + k_y^2)/2m^*$ with effective mass m^*, Fermi wave vector k_F and Brillouin zone edges at $k_y = \pm k_\mathrm{F}\cos\xi$. Because of the periodic potential, small gaps in the dispersion open up at the Brillouin zone edge, splitting the FS into distinct open and closed sections. Quasiparticles orbit around the FS with constant k_z when B lies along the interlayer direction. In very low B, because of Bragg reflection, only open orbits [Fig. 1(b)] and small closed orbits [Fig. 1(c)] occur around the distinct sections of the FS. In high B, mixing between the states on the two FS sections leads to MB at the four filled points shown in Fig. 1(a) which we term MB junctions. At these junctions a quasiparticle "tunnels" in k-space between the FS sections [12], resulting in a single large closed orbit [Fig. 1(d)].

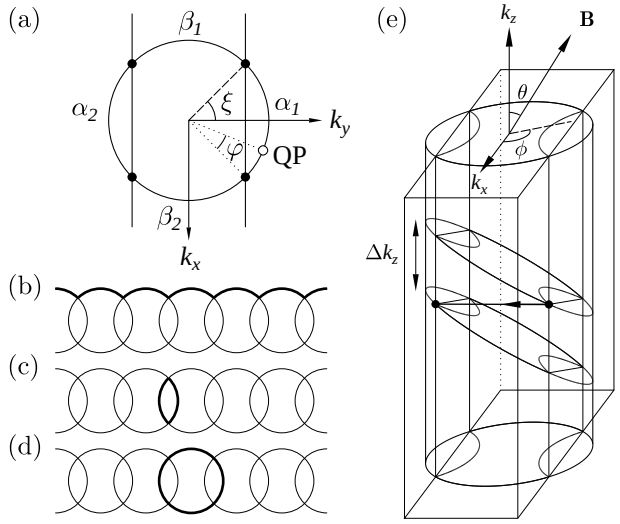

FIG. 1: (a) The Fermi surface (FS) in the k_x-k_y plane showing the points where magnetic breakdown can occur which are at $(k_x, k_y) = (\pm k_\mathrm{F}\sin\xi, \pm k_\mathrm{F}\cos\xi)$ (these are called MB junctions). The azimuthal coordinate of a quasiparticle at the point labelled QP is φ. (b) An open orbit (comprising the repeated traversal of the β_1 section). (c) Closed orbit (comprising the repeated traversal of α_1 and α_2). (d) Breakdown orbit (comprising α_1-β_1-α_2-β_2). (e) The magnetic field applied in a general direction leads to orbits which are on a cross-section perpendicular to **B**. Bragg reflection puts the quasiparticle on a different cross-section.

In fact for general values of the magnetic field there should be a *superposition* of all the orbits in Fig. 1(b)–(d) as well as many other intermediate possibilities in which MB occurs at some of the MB junctions and Bragg reflection occurs at the others. The probability $p = \exp(-B_0/B)$ of MB at each MB junction is parameterized by B_0, the characteristic breakdown field [12, 13, 14]. For all finite, non-zero values of B (for which $0 < p < 1$) there is a hierarchy of complex trajectories that must be summed to account for all possible contributions to the conductivity in which MB either does or does not occur at each MB junction. If a quasiparticle crosses N MB junctions, one has to consider 2^N possible trajectories with their correct probabilistic weightings, and this complicates a direct computation of AMROs since one has to sum over trajectories with arbitrarily long path lengths and hence arbitarily large values of N. In this Letter we describe a novel strategy to efficiently compute AMROs in a model system exhibiting MB which includes explicitly all these processes and we use it to show how different features in real data may arise. Our results are discussed in the context of recent experimental work [15] on the crystalline organic metal κ-(BEDT-TTF)$_2$Cu(NCS)$_2$ which demonstrated that, at high field, breakdown AMROs (BAMROs) could be identified in ex-

perimental data resulting from quasiparticles executing MB orbits, although until now an adequate theoretical description has been lacking.

The Boltzmann equation gives the interlayer conductivity $\sigma_{zz} = e^2\tau g(E_{\rm F})\langle v_z \bar{v_z}\rangle_{\rm FS}$ as an integral over the FS, where $\bar{v_z} = \int_0^\infty \tau^{-1}{\rm e}^{-t/\tau} v_z[\mathbf{k}(t)]\,{\rm d}t$ and $g(E_{\rm F})$ is the density of states at the Fermi energy. Our model considers the FS shown in Fig. 1(a) but includes a very weak interlayer warping so that $E(k) = \hbar^2(k_x^2 + k_y^2)/2m^* - 2t_\perp \cos k_z d_\perp$, where $d_\perp$ is the interlayer spacing and the interlayer hopping $t_\perp$ is small ($t_\perp \ll \hbar k_{\rm F}/d_\perp$). For brevity, we will henceforth write wave vectors in units of $d_\perp^{-1}$ and conductivity in units of $e^2 t_\perp^2 m^* d_\perp/\hbar^4\pi^2\omega$ so that they are dimensionless. With $\mathbf{B} = B(\sin\theta\cos\phi, \sin\theta\sin\phi, \cos\theta)$ quasiparticle orbits lie in a plane perpendicular to $\mathbf{B}$ with angular frequency given by $\omega = \omega_{\rm c}\cos\theta = eB\cos\theta/m^*$. Neglecting the influence of $t_\perp$ on the quasiparticle motion (which is only relevant for $\theta \approx 90°$), an orbit can be described by $k_z(t) = k_z^0 + \eta\cos(\varphi - \phi + \frac{\pi}{2} - \xi)$ where φ is the azimuthal position of the quasiparticle, given at time t by $\varphi = \varphi_0 + \omega t$, and $\eta = k_{\rm F}\tan\theta$. For later convenience, we measure the azimuthal angle φ anticlockwise from the α_1-β_2 MB junction [as shown in Fig. 1(a)]. The interplanar velocity $v_z(t)$, which is needed to compute σ_{zz}, can be written in our units as $v_z(t) = \sin[k_z(t)]$.

When Bragg reflection occurs for a tilted orbit [see Fig. 1(e)] the value of k_z^0 jumps by $\Delta k_z = 2\eta\sin\phi\cos\xi$ since only the k_y value of the quasiparticle momentum changes and hence the quasiparticle continues its orbit on a *different* "slice" of the Fermi surface. We can therefore write $\sigma_{zz} = \frac{1}{\pi}\int_{-\pi}^{\pi}{\rm d}k_z^0 \int_0^{2\pi}{\rm d}\varphi_0 \sin[k_z(0)] \int_{\varphi_0}^{\infty}{\rm d}\varphi {\rm e}^{-(\varphi-\varphi_0)/\omega\tau}\sin[k_z(t)]$ where

$$k_z(t) = k_z^0 + \mathsf{n}(\varphi)\Delta k_z + \eta\cos(\varphi - \phi + \frac{\pi}{2} - \xi), \qquad (1)$$

and where the term $\mathsf{n}(\varphi)\Delta k_z$ accounts for jumps in the value of k_z^0 which occur during Bragg reflection and we set $\mathsf{n}(\varphi_0) = 0$. The k_z^0 dependence can be easily integrated out and we obtain

$$\sigma_{zz} = \int_0^{2\pi} d\varphi_0 E_+(\varphi_0) \int_{\varphi_0}^{\infty} d\varphi E_-(\varphi) e^{-{\rm i}\mathsf{n}(\varphi)\Delta k_z}, \qquad (2)$$

where the functions $E_\pm(x)$ are defined by

$$E_\pm(x) = e^{\pm{\rm i}\eta\cos(x-\phi+\frac{\pi}{2}-\xi)\pm x/\omega\tau}. \qquad (3)$$

Eq. (2) yields a real expression for σ_{zz} (one can show straightforwardly that ${\rm Im}\sigma_{zz} = 0$). However, what makes Eq. (2) challenging to evaluate is that the integrand changes depending on the path taken by the quasiparticle which, at each MB junction of the orbit, can either undergo MB tunneling (with probability $p \equiv {\rm e}^{-B_0/B\cos\theta}$) or Bragg reflection (with probability $q = 1 - p$): this information is encoded in the function $\mathsf{n}(\varphi)$ which remains constant for MB but changes by ± 1 for Bragg reflection.

A fruitful strategy is to follow separately the motion of particles starting in the four different segments of the orbit, only finally summing their contributions. We therefore write Eq. (2) as a scalar product of vectors

$$\sigma_{zz} = \boldsymbol{\lambda}_+ \cdot (\boldsymbol{\lambda}_{\rm init} + \mathbf{x}_0 - \boldsymbol{\lambda}_-), \qquad (4)$$

where $\boldsymbol{\lambda}_+$ takes care of summing up all the initial positions, $\mathbf{x}_0$ handles the MB junctions, $\boldsymbol{\lambda}_{\rm init}$ describes the initial stage of the motion up to a MB junction and $\boldsymbol{\lambda}_-$ describes contributions between MB junctions. In Eq. (4) we define

$$\boldsymbol{\lambda}_\pm = \begin{pmatrix} \lambda_\pm^{\alpha_1} \\ \lambda_\pm^{\beta_1} \\ \lambda_\pm^{\alpha_2} \\ \lambda_\pm^{\beta_2} \end{pmatrix} = \begin{pmatrix} \int_0^{2\xi} d\varphi_0 E_\pm(\varphi_0) \\ e^{\mp 2\xi/\omega\tau}\int_{2\xi}^{\pi} d\varphi_0 E_\pm(\varphi_0) \\ e^{\mp\pi/\omega\tau}\int_{\pi}^{\pi+2\xi} d\varphi_0 E_\pm(\varphi_0) \\ e^{\mp(\pi+2\xi)/\omega\tau}\int_{\pi+2\xi}^{2\pi} d\varphi_0 E_\pm(\varphi_0) \end{pmatrix},$$

$$\boldsymbol{\lambda}_{\rm init} = \begin{pmatrix} \int_{\varphi_0}^{2\xi} d\varphi E_-(\varphi) \\ e^{2\xi/\omega\tau}\int_{\varphi_0}^{\pi} d\varphi E_-(\varphi) \\ e^{\pi/\omega\tau}\int_{\varphi_0}^{\pi+2\xi} d\varphi E_-(\varphi) \\ e^{(\pi+2\xi)/\omega\tau}\int_{\varphi_0}^{2\pi} d\varphi E_-(\varphi) \end{pmatrix}, \qquad (5)$$

and $\mathbf{x}_0$ is a special case of the vector

$$\mathbf{x}_n = \begin{pmatrix} \alpha_1^n \\ \beta_1^n \\ \alpha_2^n \\ \beta_2^n \end{pmatrix}, \qquad (6)$$

representing the contribution at the MB junctions on the nth slice of the FS, where n is one of the integer value taken by the function $\mathsf{n}(\varphi)$.

Each component of the vectors $\boldsymbol{\lambda}_\pm$ and $\boldsymbol{\lambda}_{\rm init}$ contributes for a specific segment of the orbit and the exponential factors multiplying some of the components are present in order to cancel the initial exponential damping of the integrand. This damping does not depend on a specific segment but it depends on the length of trajectory before reaching this specific segment. This exponential damping is taken into account in the vector $\mathbf{x}_0$. This vector dictates the evolution of the quasiparticle's path and includes all the processes at the MB junctions. The components of the vector $\mathbf{x}_n$ are as follows:

$$\alpha_1^n = \lambda_-^{\alpha_1} e^{-{\rm i}n\Delta k_z} + ap\beta_1^n + aq\alpha_2^{n+1}, \qquad (7)$$

$$\beta_1^n = \lambda_-^{\beta_1} e^{-{\rm i}n\Delta k_z} + bp\alpha_2^n + bq\beta_1^{n-1}, \qquad (8)$$

$$\alpha_2^n = \lambda_-^{\alpha_2} e^{-{\rm i}n\Delta k_z} + ap\beta_2^n + aq\alpha_1^{n-1}, \qquad (9)$$

$$\beta_2^n = \lambda_-^{\beta_2} e^{-{\rm i}n\Delta k_z} + bp\alpha_1^n + bq\beta_2^{n+1}, \qquad (10)$$

where $a = \exp(-2\xi/\omega\tau)$ and $b = \exp(-(\pi - 2\xi)/\omega\tau)$ are the increments in the damping exponential after traversing an α or β segment respectively. These recursive equations encode all the information about the behaviour at

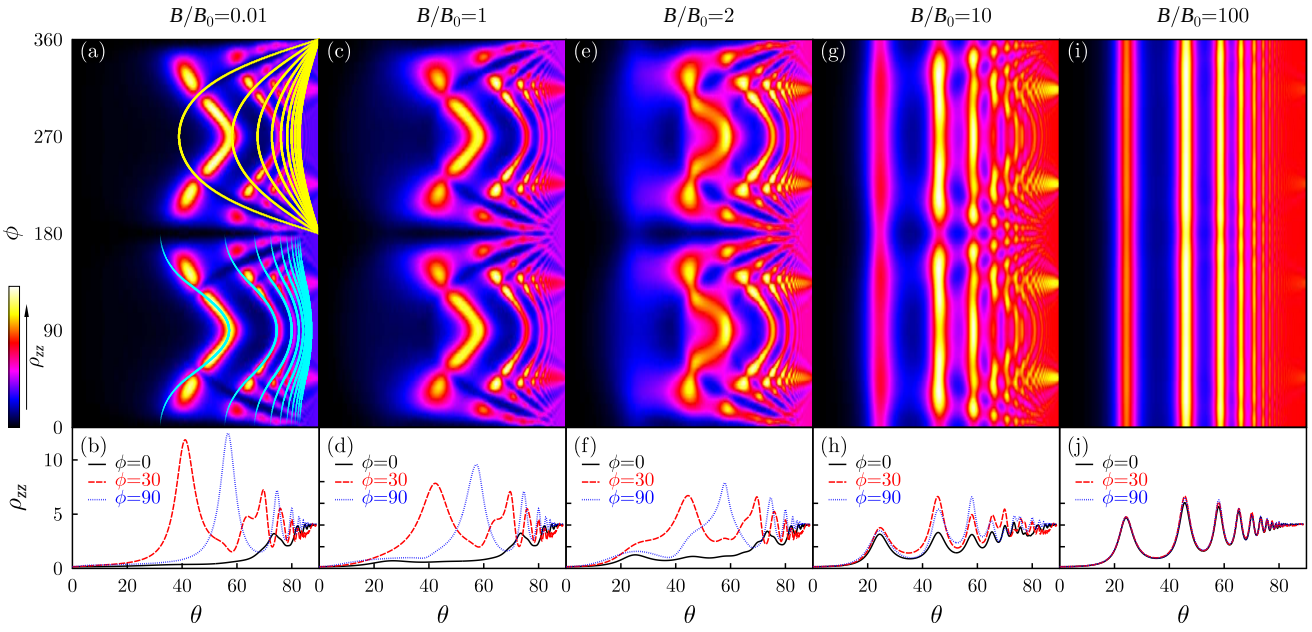

FIG. 2: Calculated resistivity as a function of ϕ and θ for different values of B/B_0. In these simulations, the parameters are chosen to conform approximately to those appropriate for experiments on κ-(BEDT-TTF)$_2$Cu(NCS)$_2$($m^* = 5m_e$, $B = 45\,\mathrm{T}$, $\tau = 3\,\mathrm{ps}$), see [15, 16]. The yellow lines in (a) show the expected minima for Lebed oscillations and the blue lines show the expected maxima for Yamaji oscillations.

the MB junctions. Because $x_{n\pm1} = x_n e^{\mp \mathrm{i}\Delta k_z}$ we can write them as a single vector equation

$$\mathbf{x}_n = \boldsymbol{\lambda}_- e^{-\mathrm{i}n\Delta k_z} + \underline{\underline{\mathbf{\Gamma}}}\mathbf{x}_n, \tag{11}$$

where $\mathbf{x}_n = (\alpha_1^n, \beta_1^n, \alpha_2^n, \beta_2^n)$ and the matrix $\underline{\underline{\mathbf{\Gamma}}}$ is given by a product of two matrices, one describing damping and the other taking into account the connection between orbit segments:

$$\underline{\underline{\mathbf{\Gamma}}} = \begin{pmatrix} a & 0 & 0 & 0 \\ 0 & b & 0 & 0 \\ 0 & 0 & a & 0 \\ 0 & 0 & 0 & b \end{pmatrix} \begin{pmatrix} 0 & p & qe^{-\mathrm{i}\Delta k_z} & 0 \\ 0 & qe^{\mathrm{i}\Delta k_z} & p & 0 \\ qe^{\mathrm{i}\Delta k_z} & 0 & 0 & p \\ p & 0 & 0 & qe^{-\mathrm{i}\Delta k_z} \end{pmatrix}. \tag{12}$$

Eq. (11) is readily solved by assigning $n = 0$ to the FS slice initially occupied by the quasiparticle. Thus with $\mathbf{x}_0 = (\underline{\underline{\mathbf{I}}} - \underline{\underline{\mathbf{\Gamma}}})^{-1}\boldsymbol{\lambda}_-$, where I is 4×4 identity matrix, we obtain

$$\sigma_{zz} = \boldsymbol{\lambda}_+ \cdot \boldsymbol{\lambda}_{\mathrm{init}} + \boldsymbol{\lambda}_+ \cdot \underline{\underline{\mathbf{\Gamma}}}(\underline{\underline{\mathbf{I}}} - \underline{\underline{\mathbf{\Gamma}}})^{-1} \cdot \boldsymbol{\lambda}_-, \tag{13}$$

which is the main result of this paper. The expression for the $\underline{\underline{\mathbf{\Gamma}}}(\underline{\underline{\mathbf{I}}} - \underline{\underline{\mathbf{\Gamma}}})^{-1}$ matrix is:

$$\underline{\underline{\mathbf{\Gamma}}}(\underline{\underline{\mathbf{I}}} - \underline{\underline{\mathbf{\Gamma}}})^{-1} = \frac{1}{N}\begin{pmatrix} t & apr^* & ar^*s^* & a^2ps^* \\ abps & w & bpr^* & abp^2 \\ ars & a^2ps & t & apr \\ bpr & abp^2 & abps^* & w^* \end{pmatrix}, \tag{14}$$

where $N = 1 + b^2q^2 - a^2(q^2 + b^2(p^2 - q^2)^2) - 2bq(1 + a^2(p^2 - q^2))\cos\Delta k_z$ and

$$r = 1 - be^{\mathrm{i}\Delta k_z}q \tag{15}$$
$$s = e^{\mathrm{i}\Delta k_z}q + b(p^2 - q^2) \tag{16}$$
$$t = 1 + b^2q^2 - 2bq\cos\Delta k_z - N \tag{17}$$
$$w = b(qe^{\mathrm{i}\Delta k_z}r^* + a^2(p^2 - q^2)s). \tag{18}$$

The integrals in Eq. (5) can be evaluated using the Jacobi-Anger expansion $e^{\mathrm{i}z\cos\theta} = \sum_{k=-\infty}^{\infty} \mathrm{i}^k J_k(z)e^{\mathrm{i}k\theta}$ where $J_k(z)$ is a k-th order Bessel function of the first kind and hence $\int E_\pm(\theta)d\theta = \sum_{k=-\infty}^{\infty} \mathrm{i}^k J_k(\pm\eta)z_k^\pm e^{\theta(\mathrm{i}k\pm 1/\omega\tau)}$, where $z_k^\pm = e^{-\mathrm{i}k(\phi - \frac{\pi}{2} + \xi)}/(\mathrm{i}k \pm 1/\omega\tau)$. This implies that

$$\boldsymbol{\lambda}_\pm = \sum_{k=-\infty}^{\infty} \mathrm{i}^k z_k^\pm \begin{pmatrix} J_k(\pm\eta)(e^{2\mathrm{i}k\xi}e^{\pm 2\xi/\omega\tau} - 1) \\ J_k(\pm\eta)((-1)^k e^{\pm(\pi - 2\xi)/\omega\tau} - e^{2\mathrm{i}k\xi}) \\ J_k(\mp\eta)(e^{2\mathrm{i}k\xi}e^{\pm 2\xi/\omega\tau} - 1) \\ J_k(\mp\eta)((-1)^k e^{\pm(\pi - 2\xi)/\omega\tau} - e^{2\mathrm{i}k\xi}) \end{pmatrix}, \tag{19}$$

and similar techniques can be used to evaluate $\boldsymbol{\lambda}_{\mathrm{init}}$. Our results reduce to the expressions given by Yagi *et al.* [8] when $p \to 1$ or $\xi \to \frac{\pi}{2}$ while we can extract the expressions for Lebed magic angles [5] and Yamaji maxima [7] when $p \to 0$. To study the general case, we have encoded the solution in a computer program, separating each term contributing to Eq. (13) into real and imaginary parts, and have summed up the Bessel functions in Eq. (19), truncating the series at small enough J_k; this involves typically about 200 Bessel functions in the sum.

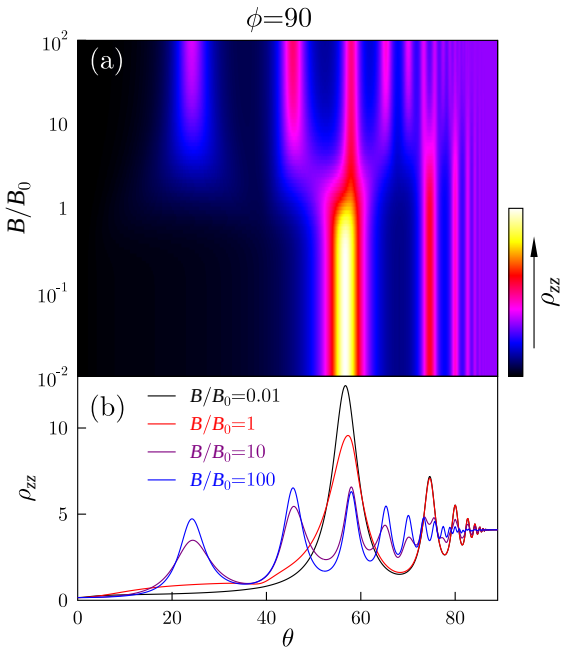

FIG. 3: Calculated resistivity as a function of B/B_0 for $\phi = 90^\circ$ for the same parameters as in Fig. 2.

In Fig. 2 we show the calculated resistivity as a function of ϕ and θ for different values of B/B_0 using parameters chosen to conform approximately to those appropriate for experiments on κ-(BEDT-TTF)$_2$Cu(NCS)$_2$. In these calculations B, τ, and hence $\omega_c\tau$, are fixed and only B_0 is varied. When B_0 is very large (small B/B_0), no MB occurs and the calculated ρ_{zz} shown in Fig. 2(a,b) display a rich structure comprising features originating from both open and closed orbits. Some of the minima are due to Lebed oscillations [5] resulting from the open orbits [see Fig. 1(b)] and their expected angular dependence is shown in the yellow lines in the upper part of Fig. 2(a) and is given by $\tan\theta = n\pi/k_F \cos\xi \sin\phi$, for integer $n \geq 1$ [5]. Some of the maxima are due to Yamaji oscillations [7, 8, 17] resulting from the lens-like closed orbits [see Fig. 1(c)] as shown in the blue lines in the lower part of Fig. 2(a). The angular positions of these are known to be given by a "caliper" measurement of the FS [18] which a simple calculation can translate into the present geometry as

$$\tan\theta \approx \frac{\pi(n-\frac{1}{4})}{k_F} \times \begin{cases} (1-\sin\phi\cos\xi)^{-1} & |\phi - \frac{\pi}{2}| < \xi \\ (\cos\phi\sin\xi)^{-1} & \text{otherwise.} \end{cases} \quad (20)$$

The values of ϕ at which either the Lebed or Yamaji oscillations dominate the calculated resistivity in Fig. 2 are similar to those found experimentally in κ-(BEDT-TTF)$_2$Cu(NCS)$_2$[16].

As B_0 decreases this structure begins to break up as MB starts to occur and in the limit of low B_0 (see Fig. 2(i,j)) the only dominant orbits are breakdown orbits (see Fig. 1(d)) leading to the observation of ϕ-independent Yamaji oscillations with maxima at $\tan\theta \approx \pi(n-\frac{1}{4})/k_F$. Because the breakdown probability is $e^{-B_0/B\cos\theta}$, it is noticeable [particularly in Figs. 2(h) and 2(j)] that ρ_{zz} is more ϕ-independent at low θ than at high θ since MB becomes less likely as θ increases. We note that at low-fields it is also possible to observe Danner-Chaikin-like oscillations [9] from the open sections close to $\phi = 0$ and $\theta = \frac{\pi}{2}$.

The transition between the low-field and high-field behavior can be studied by fixing ϕ and varying B/B_0 and this is shown in Fig. 3. The series of Yamaji maxima (starting at $\theta \approx 55^\circ$), which dominates the response at low B/B_0 due to the small lens-like orbit in Fig. 1(c), give way at high B/B_0 to a different series of Yamaji maxima (starting at $\theta \approx 23^\circ$) due to BAMROs resulting from the breakdown orbit in Fig. 1(d). The crossover between the two regimes begins above $B/B_0 \approx 1$ which is when the probability of MB becomes significant.

There is a remarkable similarity between the predictions of this model and the data of Ref. 15, 16. It is expected that this approach to summing all the contributions to the MB network model will open up new avenues in research on low-dimensional metals.

We thank EPSRC (AN) and the Oxford University Glasstone Fund (PAG) for financial support.

* Current address: Trinity College, Cambridge, CB2 1TQ, United Kingdom
† Corresponding author: s.blundell@physics.ox.ac.uk

[1] M. V. Kartsovnik, Chem. Rev. **104**, 5737 (2004).
[2] E. Ohmichi, Y. Maeno and T. Ishiguro, J. Phys. Soc. Jpn **68**, 24 (1999).
[3] M. Kawamura *et al.*, Physica B **249-251**, 882 (1998).
[4] N. E. Hussey *et al.*, Nature, **425**, 814 (2003).
[5] A. G. Lebed, JETP Lett. 43, 174 (1986).
[6] M. V. Kartsovnik, P. A. Kononovich, V. N. Laukhin and I. F. Shchegolev, JETP Lett. **48**, 541 (1988).
[7] K. Yamaji, J. Phys. Soc. Japan, **58**, 1520 (1989).
[8] R. Yagi, Y. Iye, T. Osada and S. Kagoshima, J. Phys. Soc. Jpn. **59**, 3069 (1990). Synth. Met., **41-43**, 2237 (1991).
[9] G. M. Danner, W. Kang and P. M. Chaikin, Phys. Rev. Lett., **72**, 3714 (1994).
[10] S. J. Blundell and J. Singleton, Phys. Rev. B., **53**, 5609 (1996).
[11] W. Kang, T. Osada, Y. J. Jo, and H. Kang, Phys. Rev. Lett. 99, 017002 (2007).
[12] A. B. Pippard, Phil. Trans. Roy., Soc. A **270**, 1 (1962).
[13] N. Harrison, J. Caulfield, J. Singleton, P. H. P. Reinders, F. Herlach, W. Hayes, M. Kurmoo and P. Day, J. Phys.: Condens. Matter **8**, 5415 (1996).
[14] D. Shoenberg, *Magnetic Oscillations in Metals*, (Cambridge University Press, Cambridge, 1984).
[15] A. F. Bangura, P. A. Goddard, J. Singleton, S. W. Tozer,

A. I. Coldea, A. Ardavan, R. D. McDonald, S. J. Blundell and J. A. Schlueter, Phys. Rev. B **76**, 052510 (2007).
[16] P. A. Goddard *et al.*, Phys. Rev. B., **69**, 174509 (2004).
[17] R. H. McKenzie and P. Moses, Phys. Rev. Lett. **81**, 4492 (1998).
[18] M. V. Kartsovnik, V. N. Laukhin, S. I. Pesotskii, I. F. Schegolev and V. M. Yakovenko, J. Phys. (France) I **2**, 89 (1992).